Exact scaling in competitive growth models

L. A. Braunstein[1,3] and Chi-Hang Lam[2]
[1]*Departamento de Física, Facultad de Ciencias Exactas y Naturales, Universidad Nacional de Mar del Plata, Funes 3350, 7600 Mar del Plata, Argentina*
[2]*Department of Applied Physics, Hong Kong Polytechnic University, Hung Hom, Hong Kong, China*
[3]*Center for Polymer Studies and Department of Physics, Boston University, Boston, Massachusetts 02215, USA*
(Received 31 March 2005; published 24 August 2005)

A competitive growth model (CGM) describes the aggregation of a single type of particle under two different growth rules with occurrence probabilities p and $1-p$. We explain the origin of the scaling behavior of the resulting surface roughness at small p for two CGM's which describe random deposition (RD) competing with ballistic deposition and RD competing with the Edward-Wilkinson (EW) growth rule. Exact scaling exponents are derived. The scaling behavior of the coefficients in the corresponding continuum equations are also deduced. Furthermore, we suggest that, in some CGM's, the p dependence on the coefficients of the continuum equation that represents their universality class can be nontrivial. In some cases, the process cannot be represented by a unique universality class. In order to show this, we introduce a CGM describing RD competing with a constrained EW model. This CGM shows a transition in the scaling exponents from RD to a Kardar-Parisi-Zhang behavior when p is close to 0 and to a Edward-Wilkinson one when p is close to 1 at practical time and length scales. Our simulation results are in excellent agreement with the analytic predictions.

DOI: 10.1103/PhysRevE.72.026128 PACS number(s): 89.75.Da, 81.15.Aa, 68.35.Ct, 05.10.Gg

I. INTRODUCTION

Evolving interfaces or surfaces are of great interest due to their potential technological applications. These interfaces can be found in many physical, chemical, and biological processes. Examples include film growth either by vapor deposition or chemical deposition [1], bacterial colony growth [2], and propagation of forest fires [3].

For a system exhibiting dynamical scaling, the rms roughness W of an interface is characterized by the following scaling with respect to time t and the lateral system size L:

$$W(L,t) \sim L^{\alpha} f(t/L^{z}),$$

where the scaling function $f(u)$ behaves as $f(u) \sim u^{\beta}$ with $\beta = z/\alpha$ for $u \ll 1$ and $f(u) \sim$ const for $u \gg 1$. The exponent α is the roughness exponent that describes the behavior of the saturated surface roughness with L, while the growth exponent β describes scaling at an early stage when finite-size effects are negligible. The crossover time between the two regimes is $t_s = L^z$.

A widely studied phenomenological equation representing the nonequilibrium growth of such interfaces is the Kardar-Parisi-Zhang (KPZ) equation, which in $1+1$ dimensions is given by

$$\frac{\partial h(x,t)}{\partial t} = \nu \frac{\partial^2 h(x,t)}{\partial^2 x} + \lambda \left(\frac{\partial h(x,t)}{\partial x} \right)^2 + \eta(x,t), \qquad (1)$$

where $h(x,t)$ is the local surface height at the position x and time t. The coefficients ν and λ represent the strength of the linear and nonlinear terms, respectively. The noise $\eta(x,t)$ is Gaussian with zero variance and covariance

$$\langle \eta(x,t)\, \eta(x',t') \rangle = 2D \delta(x-x')\, \delta(t-t'),$$

where D is the strength of the noise. The exponents characterizing the KPZ equation in a highly nonlinear strong coupling are $\alpha = 1/2$ and $\beta = 1/3$. In contrast, when $\lambda = 0$ the linear Edward-Wilkinson (EW) equation is recovered, leading to the weak-coupling exponents $\alpha = 1/2$ and $\beta = 1/4$. When both ν and λ are zero the growth reduces to a simple random deposition (RD) with $\beta = 1/2$ but lacks a saturation regime.

There has been a recent interest in the study of competitive growth models (CGM's) analyzing the interplay and competition between two growth processes for a single surface. These CGM's are often more realistic in describing growth in real materials [4], in which more than one microscopic growth mode usually exists. For example, two distinct growth phases were observed in experiments on interfacial roughening in Hele-Shaw flows [5,6] as well as in simulations on electrophoretic deposition of polymer chains [7,8]. The resulting universalities from these competing processes are not well understood [9–13]. Recently Horowitz and Albano [10] introduced a CGM called the BD-RD model in which the microscopic growth rule follows either the ballistic deposition (BD) model with probability p or the simple RD with probability $1-p$. This system exhibits a transition at a characteristic time from RD to KPZ. For this particular CGM, they found numerically that the scaling behavior of W is giving by the empirical form

$$W \sim \frac{L^{\alpha}}{p^{\delta}} F\left(\frac{t}{p^{-y} L^{z}} \right). \qquad (2)$$

Based on numerical estimates, exact values

$$\delta = 1/2 \quad \text{and} \quad y = 1 \qquad (3)$$

have been conjectured for the BD-RD model. Based on this conjecture, the authors [10,11] concluded using scaling arguments that the model follows Eq. (1) with $\nu \sim p$ and $\lambda \sim p^{3/2}$. Subsequently, a similar CGM—namely, the EW-RD

model describing the competition between the EW and RD models [9]—has been studied. The simulations showed that Eq. (2) also holds with a different set of exponents which are conjectured to be

$$\delta = 1 \quad \text{and} \quad y = 2. \tag{4}$$

This model can also be described by Eq. (1) with $\nu \sim p^2$ and $\lambda = 0$ [9,12]. In these CGM's, the choice of the growth rule is independent of the lattice position. More recently, another CGM that combines RD with KPZ-type growth has been studied and gives different values of δ and y due to the spatial inhomogeneity in the choice of the growth rules. [14]

In this paper, we explain the scaling form (2) for the BD-RD and EW-RD models and derive rigorously the exact exponents δ and y for small p using simple arguments. In addition, from the above examples of CGM's, one might be tempted to conclude that a CGM based on RD and a model in the KPZ (EW) universality class should always lead to an overall process in the KPZ (EW) class. We suggest that these naive predictions of universality are not always correct. Close examination of the microscopic details of the growth models is indeed essential. This is illustrated by introducing a constrained EW (CEW) model. Although this model essentially belongs to the EW class, a CGM in the form of the CEW-RD model at sufficiently small p results in an overall process in the KPZ universality class. Our model also demonstrates that a CGM can crossover from one universality class to another by tuning p.

II. EXACT SCALINGS FOR CGM's

In the RD model, a particle is dropped at a randomly selected column. The local surface height is increased by 1. For the BD-RD or EW-RD CGM's described above, a particle is deposited on the surface following a RD process with probability $1-p$ and by another process A (which is either BD or EW) with probability p. Now, we derive analytically the exact exponents δ and y which characterize the p dependence of the scaling behavior of W given in Eq. (2). We consider $p \to 0$ (small p). At each unit time, L particles are deposited. The average time interval between any two consecutive A events at any column i is $\tau = 1/p$. During this period, $\tau - 1 \simeq \tau$ atoms on average are directly stacked onto the surface according to the simple RD rule. The local height at column i hence increases by η_i which is an independent Gaussian variable with mean $\bar{\eta} = \tau$ and standard deviation $\sigma_\eta = \sqrt{\tau}$ according to the central limit theorem. The mean, however, only leads to an irrelevant rigid shift of the whole surface. We can easily apply a vertical translation so that $\bar{\eta} = 0$. After these τ RD events at column i, one A event on average is expected at the same column.

Now we consider A to be the BD process. The CGM is then the BD-RD model. When a BD event occurs at column i, its height is updated in the simulations according to $h_i \to \max\{h_{i-1}, h_{i+1}, h_i + 1\}$. In the limit of small $p (\sigma_\eta \gg 1)$ the height of the atom is negligible compared with the increments due to the RD events. The growth rule hence reduces to

$$h_i \to \max\{h_{i-1}, h_{i+1}, h_i\}. \tag{5}$$

We have now arrived at a limiting BD-RD model defined as follows: At every coarsened time step $\tau = 1/p$, the local height h_i at every column i first changes by an additive Gaussian noise term η_i with mean zero and standard deviation $\sigma_\eta = \sqrt{\tau}$. Then the limiting BD growth rule in Eq. (5) is applied to every column i. A more careful analysis should account for the fact that the BD events at various columns indeed occur randomly and asynchronously during period τ. But this does not affect our result. In this limiting model, time and vertical length scales are determined completely by τ and σ_η, respectively. Therefore, time scales as $t \sim \tau = 1/p$ while roughness scales as $W \sim \sigma_\eta \sim 1/p^{1/2}$. This explains the p dependence of the scaling form in Eq. (2). In particular, we obtain the exact exponents $y = 1$ and $\delta = 1/2$ in agreement with values in Eq. (3) first conjectured in Ref. [10] but *not* derived analytically before.

Next, we assume that A represents the EW growth rule instead. For this growth rule, a particle is dropped at a random column but when it reaches the surface it is allowed to relax to the lower of the nearest-neighboring columns. If the heights at both nearest neighbors are lower than the selected one, the relaxation is directed to either of them with equal probability. Our CGM now becomes a EW-RD model. The corresponding derivation of the characteristic length and time scales is similar to the BD-RD case. Assuming again small p, the average time interval between any two consecutive EW events at any given site is $\tau = 1/p$. Consider a characteristic time $n\tau$. On average $n\tau$ RD events occur at any given site, leading to height increments with a standard deviation $\sqrt{n\tau}$. However, only n EW events take place. The resulting smoothing dynamics is such that a big step, for instance, will typically decrease the height by n. For scaling to hold, there can only be one unique relevant length scale in the vertical direction. The two length scales $\sqrt{n\tau}$ and n hence have to be proportional to each other. Then we obtain $\tau \sim n$. The characteristic time scale considered is hence $n\tau \sim 1/p^2$, while a characteristic length scale for the surface height is $\sqrt{n\tau} \sim 1/p$. We have hence derived $y = 2$ and $\delta = 1$ [see Eq. (4)] previously conjectured in Ref. [9]. The extended scaling form and scaling exponents derived are exact for $p \to 0$. At finite p, we expect deviations from the exact scalings which indeed were observed numerically [10]. Note that the deviations cannot be caused by the finite lattice size according to our analytic calculations above.

III. CEW AND CEW-RD MODELS

We now introduce the CEW model which is a generalization of the EW model. In $1+1$ dimensions, particles are aggregated by the following rules. We choose a site i at random among the L possible sites. The surface height h_i at the selected column is increased by 1 if its height is lower than the values $h_{i\pm1}$ at the neighboring columns. Otherwise, either h_{i-1} or h_{i+1}, whichever smaller, is increased to

$$h_{i\pm1} = \max\{h_{i\pm1} + 1, h_i - c\}. \tag{6}$$

If $h_{i-1} = h_{i+1}$, either one will be updated with equal probability. Here, c is a tuning parameter. Growth at $i \pm 1$ physically

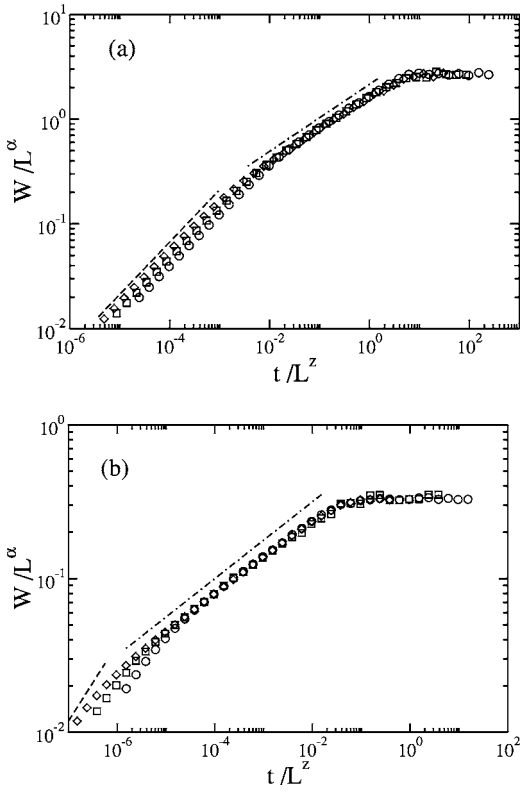

FIG. 1. log-log plot of W/L^{α} as a function of t/L^{z} for $c=4$ and different L values: $L=256$ (○), $L=512$ (□), $L=1024$ (◇). (a) The scaling exponents used here are characteristic of the KPZ equation $\alpha=1/2$ and $z=3/2$. Here $p=0.02$. The dashed line with slope 1/2 and the dot-dashed line with slope 1/3 are used has a guide to show the RD and KPZ regimes, respectively. (b) The same as (a) but for $p=0.64$, with $\alpha=1/2$ and $z=2$, characteristic of the EW behavior. The dashed line with slope 1/2 and the dot-dashed line with slope 1/4 are used has a guide to show the RD and EW regimes, respectively.

represents the rollover of a newly dropped particle to a lower site nearby under the influence of gravity, for example. In the original EW model, there is no limit in the vertical distance transversed during the rollover and the particle can in principle slides down a very deep cliff if one exists next to column i. This is unphysical if there is a finite chance for the sideway sticking of the particle to the cliff. In the CEW growth rule defined in Eq. (6), this vertical drop during rollover is limited to c by the process of sideway sticking. As $c\to\infty$, it is easy to see that CEW reduces to the standard EW model. At $c=0$, sideway sticking of particles occurs frequently and CEW behaves similarly to BD, although the precise growth rules are different. In the rest of this paper, we use $c=4$.

To be demonstrated by the simulations presented later, the CEW model at $c=4$ at practical length and time scales considered here ($L\leqslant 8192$ and $t\leqslant 10^{7}$) belongs to the EW universality class. Finally, we define the CEW-RD model which is a CGM based on the RD and CEW models. Similar to the definitions of other CGM's defined above, at each time step, the CEW growth rule is applied with probability p while a RD event occurs with probability $1-p$. Time t is then increased by $1/L$.

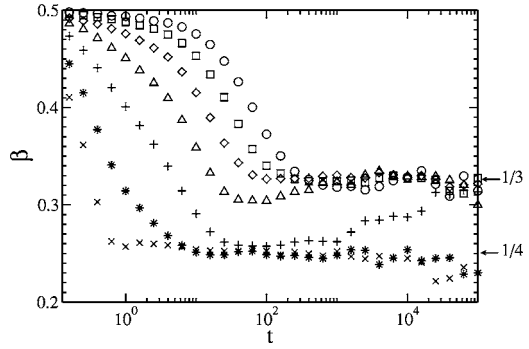

FIG. 2. Plot of the growth exponent β as a function of $\log t$ for $L=8192$ and different p values: $p=0.02$ (○), $p=0.04$ (□), $p=0.08$ (◇), $p=0.16$ (△), $p=0.32$ (+), $p=0.64$ (∗), and $p=1.0$ (×) showing the change in the behavior of β with time. The β values where computed over 100 realizations. The arrows are used as guides to show the asymptotic exponents.

Now, we present the simulation results. In Figs. 1(a) and 1(b), we show the log-log plot of W/L^{α} as a function of t/L^{z} for two limiting values of p. For small p, the behavior is consistent with the KPZ universality class with $\alpha=1/2$ and $z=3/2$, while for p close to 1 the system behaves as predicted by the EW equation with $\alpha=1/2$ and $z=2$. The initial regime corresponding to the RD deposition, with $\beta=1/2$, does not scale with the system size. In order to show that the universality class depends on p, we compute β as a function of t using successive slopes defined in Ref. [15].

In Fig. 2 we plot β as a function of $\log t$ for different values of p. At the beginning $\beta=1/2$ as expected for the initial RD regime. After this early regime, the system evolves either to the KPZ class with $\beta=1/3$ for small p or to the EW class for large p with $\beta=1/4$. For intermediate p values (after the RD regime), the system behaves as in the weak coupling of Eq. (1). It is easy to observe a transition from an EW to a KPZ-class for $p\geqslant 0.32$ while for small p, the system always belongs to the KPZ universality class.

IV. GENERALIZED CONTINUUM EQUATIONS AND SCALING

As shown above the CEW-RD model has a transition from a KPZ to a EW class as the tuning parameter p goes from 0 to 1. Thus the nonlinear coefficient λ of the KPZ equation has to vanish as $p\to 1$. In order to understand the functional form of $\lambda(p)$, we perform a finite-size scaling analysis of the growth velocity v used on Ref. [16],

$$\Delta v(L)\sim \lambda L^{-\alpha} \quad \text{for } t\gg t_{s}, \tag{7}$$

where $\Delta v(L,t)=v(L=1024,t)-v(L=10,t)$ and $v(L,t)=\langle dh/dt\rangle$. Here $\langle\cdots\rangle$ denotes the average over L an over different configurations. The Δv correction should go to zero when the nonlinear term λ vanishes.

Thus, using Eq. (7), we can determine how λ in the KPZ equation depends on p. In Fig. 3 we plot Δv as a function of p for fixed L to show the p dependence of λ. From the plot, we can see that the functional form for the CEW-RD CGM is totally different from the scaling form $\lambda(p)\sim p^{3/2}$ of the

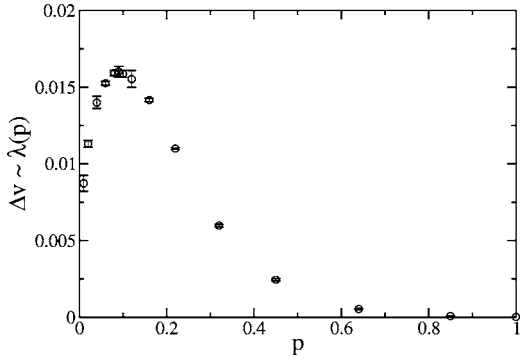

FIG. 3. Linear plot of $\Delta v \sim \lambda$ as a function of p, where $\Delta v(L,t)=v(L=1024,t)-v(L=10,t)$. The averages where taken over typically 500 realizations. The errors bars where computed using 5 independent sets of 500 realizations each.

BD-RD model [10]. For small p values, λ has a power-law dependence with p, while for large p, $\lambda(p)\to 0$ with a fast decay. Now we proceed to generalize Eq. (1) for a CGM applying the following transformation: $h'=hf(p)b^{\alpha}$, $x'=bx$, and $t'=g(p)tb^{z}$, where b is the lateral length transformation. As the interface evolution of these CGM's is independent of b, they can be described, after applying the transformations defined above, by the generalized continuum equation

$$\frac{\partial h(x,t)}{\partial t} = \nu(p)\frac{\partial^2 h(x,t)}{\partial^2 x} + \lambda(p)\left(\frac{\partial h(x,t)}{\partial x}\right)^2 + D(p)\,\eta(x,t), \tag{8}$$

with

$$\nu(p) = \nu_0 g(p), \tag{9}$$

$$\lambda(p) = \lambda_0 f(p) g(p), \tag{10}$$

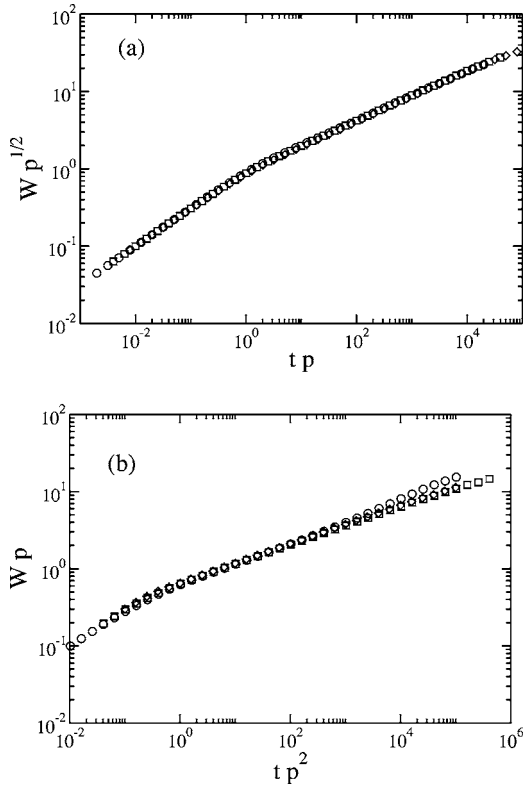

FIG. 4. log-log plot of $Wf(p)$ as a function of $tg(p)$ for $L=8192$ and different p values. In (a) $p=0.02$ (○), $p=0.04$ (□), and $p=0.08$ (◇), $g(p)=p$ and $f(p)=p^{1/2}$. In (b) $p=0.32$ (○), $p=0.64$ (□), and $p=1.0$ (◇), $g(p)=p^2$ and $f(p)=p$. Notice the departure from the EW scaling behavior for $p=0.32$.

$$D(p) = \frac{g(p)}{f(p)^2}, \tag{11}$$

where $g(p)$ is related to the characteristic time scale when the correlations begins to dominate the dynamic of the interface and $f(p)$ is related to the saturation length scale. Notice that for the EW universality class $\lambda_0=0$. Using the exact results from Sec. II we obtain

$$f(p) \sim \begin{cases} p^{1/2}, & \text{for the BD-RD and CEW-RD models when } p \text{ is small,} \\ p, & \text{for the CEW-RD model when } p \text{ is large,} \end{cases} \tag{12}$$

and

$$g(p) \sim \begin{cases} p, & \text{for the BD-RD and CEW-RD models when } p \text{ is small,} \\ p^2, & \text{for the CEW-RD model when } p \text{ is large,} \end{cases} \tag{13}$$

Thus Eqs. (9)–(11), can be replaced by

$$\nu(p) \sim \begin{cases} \nu_0 p, & \text{for the BD-RD and CEW-RD models when } p \text{ is small,} \\ \nu_0 p^2, & \text{for the CEW-RD model when } p \text{ is large,} \end{cases} \tag{14}$$

$$\lambda(p) \sim \begin{cases} \lambda_0 p^{3/2}, & \text{for the BD-RD model when } p \text{ is small,} \\ 0, & \text{for the CEW-RD model when } p \text{ is large,} \end{cases} \tag{15}$$

and $D(p)\sim D_0$ for the BD-RD and CEW-RD models independent of p.

Thus, for the CGM belonging to the KPZ (EW) universality class the evolution of the interface is given by

$$\frac{\partial h}{\partial t} = \begin{cases} \nu_0 p \dfrac{\partial^2 h(x,t)}{\partial^2 x} + \lambda_0 p^{3/2} \left(\dfrac{\partial h(x,t)}{\partial x} \right)^2 + \eta(x,t), & \text{for the BD-RD and CEW-RD models when } p \text{ is small,} \\ \nu_0 p^2 \dfrac{\partial^2 h(x,t)}{\partial^2 x} + \eta(x,t), & \text{for the CEW-RD model when } p \text{ is large,} \end{cases} \tag{16}$$

The scaling behavior of W [12] is then

$$Wf(p)/L^{\alpha} \sim \begin{cases} F\left(g(p)\lambda_0 \sqrt{\dfrac{D_0}{\nu_0}} \dfrac{t}{L^z} \right), & \text{for the KPZ model,} \\ F\left(g(p)\nu_0 \dfrac{t}{L^z} \right), & \text{for the EW model,} \end{cases} \tag{17}$$

which after replacing $f(p)$ and $g(p)$ given by Eqs. (12) and (13) leads to the exact scaling of W predicted by Eq. (2) with the exact values of δ and y derived in Sec. II. In Fig. 4 we show the log-log plot of $Wf(p)$ as a function of $tg(p)$ in the two limiting p values for a fixed value of L. The results are in agreement with our exact results (see Sec. II) and our scaling ansatz [Eq. (17)].

V. CONCLUSIONS

We derive analytically the p dependence in the scaling behavior in two CGM's named the BD-RD and EW-RD models. Exact scaling exponents are derived and are in agreement with previously conjectured values [9,10]. To our knowledge, these exact scaling behaviors were not analytically derived before. This derivation allows us to compute the scaling behaviors of the coefficients of the continuum equations that describe their universality classes. We introduce the CEW-RD model to show that not all CGM's can be represented by a unique universality class. The CEW-RD model is an EW model in the limit of large p at practical length and time scales, while in the other limit (small p), it follows the strong-coupling behavior of the KPZ equation. Our simulation results are in excellent agreement with the analytic predictions.

ACKNOWLEDGMENTS

L.A.B. thanks UNMdP for the financial support. C.H.L. was supported by HK RGC, Grant No. PolyU-5289/02P.

[1] F. Family, J. Phys. A **19**, L441 (1986); A.-L. Barabási and H. E. Stanley, *Fractal Concepts in Surface Growth* (Cambridge University Press, New York, 1995); P. Meakin, *Fractals, Scaling and Growth far from Equilibrium* (Cambridge University Press, Cambridge, England, 1998).
[2] E. V. Albano, R. C. Salvarezza, L. Vázquez, and A. J. Arvia, Phys. Rev. B **59**, 7354 (1999).
[3] S. Clar, B. Drossel, and F. Schwabl, J. Phys.: Condens. Matter **8**, 6803 (1996).
[4] Y. Shapir, S. Raychaudhuri, D. G. Foster, and J. Jorne, Phys. Rev. Lett. **84**, 3029 (2000).
[5] A. Hernandez-Machado, J. Soriano, A. M. Lacasta, M. A. Rodriguez, L. Ramirez-Piscina, and J. Ortin, Europhys. Lett. **55**, 194 (2001).
[6] J. Soriano, J. Ortin, and A. Hernandez-Machado, Phys. Rev. E **66**, 031603 (2002); **67**, 056308 (2003).
[7] G. M. Foo and R. B. Pandey, Phys. Rev. Lett. **80**, 3767 (1998).
[8] F. W. Bentrem, R. B. Pandey, and F. Family, Phys. Rev. E **62**, 914 (2000).
[9] C. M. Horowitz, R. A. Monetti, and E. V. Albano, Phys. Rev. E **63**, 066132 (2001).
[10] C. M. Horowitz and E. V. Albano, J. Phys. A **34**, 357 (2001).
[11] C. M. Horowitz and E. V. Albano, Eur. Phys. J. B **31**, 563–569 (2003).
[12] D. Muraca, L. A. Braunstein, and R. C. Buceta, Phys. Rev. E **69**, 065103(R) (2004).
[13] A. Chame and F. D. A. Aarão Reis, Phys. Rev. E **66**, 051104 (2002).
[14] A. Kolakowska, M. A. Novotny, and P. S. Verma, Phys. Rev. E **70**, 051602 (2004).
[15] L. A. Braunstein, S. V. Buldyrev, S. Havlin, and H. E. Stanley, Phys. Rev. E **65**, 056128 (2002).
[16] J. Krug and P. Meakin, J. Phys. A **23**, L987 (1990).